ELSEVIER

Journal of Nuclear Materials 244 (1997) 168–172

journal of nuclear materials

Nanoindentation test on electron beam-irradiated boride layer of carbon–carbon composite for plasma facing component of large Tokamak device

M. Kanari [a,1], K. Tanaka [a], S. Baba [b], M. Eto [b,*], K. Nakamura [c,2]

[a] *Department of Mechanical Engineering, Nagaoka University of Technology, Tomioka-cho 1603-1, Nagaoka, Niigata-ken 940-21, Japan*
[b] *Japan Atomic Energy Research Institute, Toaki Research Establishment, Tokai-mura, Ibaraki-ken 319-11, Japan*
[c] *Japan Atomic Energy Research Institute, Naka Fusion Research Establishment, Naka-machi, Ibaraki-ken 311-01, Japan*

Received 19 July 1996; accepted 8 November 1996

Abstract

The nanoindentation behavior of an electron irradiated boride layer overlaid on carbon–carbon (C/C) composite for plasma facing components of a large Tokamak device was examined up to the maximum load of 0.3 mN. The scanning electron micrography indicated that the irradiation caused the melt-down and resolidification of the boron carbide layer. However, it was found by the X-ray diffraction analysis that the layer did not change its crystalline structure. Young's modulus and mean pressure of the irradiated area were estimated from load–penetration depth (P–h) curves as 270 GPa and 19.2 GPa, respectively, which were 40 and 20% lower than the values for the bulk material. These properties for the unirradiated region were 125 GPa and 3.1 GPa, respectively, only one third and one tenth of the values for the bulk. It is attributed to the porous structure of the unirradiated material.

1. Introduction

Carbon materials such as isotropic graphite and carbon fiber reinforced carbon (C/C composite) material have been used as the divertor plate exposed to plasma in the present large Tokamak fusion facility (JT-60). To prevent the damage caused by plasma and the inflow of the carbon into plasma, research has been made on the converted boride layer of some hundred micrometers overlaid on the carbon material. The energy loads to the divertor tiles in the JT-60 are estimated as 10 MW/m^2 for 5 s during the normal operation and 2–3 MJ/m^2 during the plasma disruption. Tanaka et al. [1,2] fabricated a facility named JEBIS by which one can give specimens high heat flux using a high energy electron beam with a capacity of 4 A at 100 keV. Nakamura et al. [3] used the JEBIS to examine the damage on the various boride-overlaid C/C composites in two heating conditions; heat flux of 5–40 MW/m^2 for 5 s and 550 MW/m^2 for 5–10 ms in simulation of the normal operation condition and plasma disruption, respectively. They found that the irradiation caused a slight damage such as weight loss and change in boron/carbon ratio in the boride layer under the normal heating condition, while the exfoliation of boride layers occurred under the disruption condition. It is clear that the determination of mechanical properties of such damaged boride layers is essential for the design of Tokamak devices. It is also necessary to evaluate the irradiation damage caused in the layers during the operation of the Tokamak devices. For this purpose the hardness test may be one of the most convenient means since it is easily applicable in such a critical environment. However, it is practically impossible to determine the hardness of the irradiated surface layer using the conventional hardness testing technique such as Vickers hardness. This is because the irradiated layer is

* Corresponding author. Tel.: +81-29 282 5396; fax: +81-29 282 6712; e-mail: eto@cat.tokai.jaeri.go.jp.
[1] Tel.: +81-258 461 611; fax: +81-258 466 972.
[2] Tel.: +81-29 270 7555; fax: +81-29 270 7558.

PII S0022-3115(96)00728-3

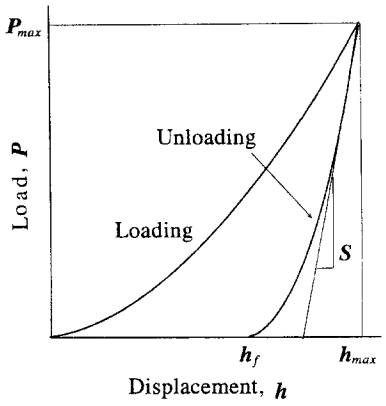

Fig. 1. Schematic representation of load versus indenter displacement data for an indentation experiment.

formed only in the order of 10 μm in thickness at the surface of the boride layer about 1 mm in thickness. Recently, particular attention has been paid to nanoindentation tests for the examination of elastic and plastic behavior of brittle materials, thin films and radiation-damaged materials [4]. In this study the Young's modulus and mean pressure (hardness) of irradiated and unirradiated boride layers are estimated by the nanoindentation test and the results are compared with those on a bulk boron carbide (B_4C).

Conventional hardness is equivalent to the real pressure under the indenter, i.e., the applied load divided by the real projected area of contact A_r. However, in the case of nanoindentation, hardness can be obtained using a depth-sensing instrument with a Berkovich indenter. A schematic load–displacement (P–h) curve for elastic–plastic behavior is represented in Fig. 1. The relevant mean pressure p_m at the maximum load is assessed as the applied load P_{max} divided by the apparent projected area of contact $A_a = 3(3)^{1/2}\tan^2\alpha(h_{max})^2$, i.e.,

$$p_m = P_{max}/A_a = 0.129\cot^2\alpha P_{max}/(h_{max})^2, \quad (1)$$

where α is the apical angle of indenter and h_{max} the maximum penetration depth. A method of determining the Young's modulus E is to correlate it with the initial unloading stiffness, $S = dP/dh$ [5–7]. The basic assumption is that during the very initial unloading of the indenter, the contact area between the indenter and the sample remains constant and behaves like a flat punch contact with an elastic half space. Sneddon's analysis on elastic contact [8] leads to

$$S = dP/dh = C_A E^* A_r^{1/2}, \quad (2)$$

where $C_A = 2/\pi^{1/2}$ for axisymmetrical punch. The effective Young's modulus E^* is expressed by

$$1/E^* = (1 - \nu^2 I)/E_I + (1 - \nu^2 S)/E_S \quad (3)$$

where ν is Poisson's ratio and subscripts I and S denote the indenter and sample, respectively. In a particular case where the material behaves elastically, the Berkovich indentation is expressed [9] by

$$P = 0.95\tan\alpha E^* h^2 \quad (4)$$

and

$$p_m = 0.813\cot\alpha E^*. \quad (5)$$

2. Experimental

The substrate C/C composite used in this study was developed for the application to the divertor of the JT-60. The composite consisted of the stacked piles of discontinuous carbon fiber felt reinforcement impregnated with a resin matrix precursor. After the compaction and carbonization, the carbon matrix was grown several times by the chemical vapor infiltration process and subsequently graphitized in a high temperature atmosphere. The fibers were arranged two dimensionally in the matrix, being crossed with each other. The boride layer on C/C composite was overlaid to 900 μm in thickness on an as-impregnated plate of 20 × 20 × 30 mm by the reduction of boron oxide at a high temperature. High heat flux tests on the material in the simulation of plasma disruption was carried out at a heat flux of 550 MW/m^2 for 2 ms using JEBIS. Bulk B_4C samples were cut from a B_4C pellet which was sintered by hot pressing of B_4C powder. Mechanical properties of the substrate C/C composite and the bulk B_4C are summarized in Table 1. Young's moduli were determined from the slope of the elastic region of the tensile stress–strain curves. Hardness value for C/C composite in the table is determined by a nanoindentation test [10] and that for the bulk B_4C by micro-Vickers hardness test at 300 gf. Indentation test in the present study was performed at $P_{max} = 0.3$ mN using a nanoindentation tester with

Table 1
Typical properties of substrate C/C composite and standard B_4C

Material	Bulk density (Mg/m^3)	True density (Mg/m^3) [a]	Young's modulus (GPa)	Hardness (GPa)
Composite	1.7	2.1	7.6	0.073
B_4C	2.35	2.5	420	31

[a] Catalogue values given by the manufacturers.

resolutions of load and displacement of 0.1 μN and 1 nm, respectively [9]. The measurement was conducted at five different points in each of the irradiated and unirradiated areas in the boride layer of C/C composite, and in the bulk B_4C. For a reference, micro-Vickers indentation on the unirradiated area was also carried out at 50 gf using a conventional Vickers hardness tester.

3. Results and discussion

3.1. Microstructure

Fig. 2 shows an optical microscopic photograph of the irradiated boride layer (a) and the sketch of the cross-section perpendicular to the indented surface (b). The bright circle at the center of the sample in Fig. 2(a) is the irradiated area of 9.8 mm in diameter, which was melted by the high heat flux and re-solidified. The irradiated surface as shown in Fig. 2(b) seems to be a crater with a pile up of 130 μm at the fringe and a sink-in of 320 μm at the center, which indicates that the morphology was formed by splashing the melted boride surface. Fig. 3 shows scanning electron micrographs (SEM) of the unirradiated area (a) and the irradiated area (b). SEM image of the unirradiated area in Fig. 3(a) (the dark region in Fig. 2(a)) reveals that the crystallized grains of about 1.5 μm are bridged over each other, but the density of the area looks low because of the presence of the large amount of pores. The irradiated area in Fig. 3(b) is found to be agglomerated by the resolidification and the flaky grains grow inhomogeneously to the sizes ranging from 7 to 30 μm. The thickness of the resolidified region was found to be about 40 μm from the SEM observations on the cross-section of the region, which is schematically represented in Fig. 2(b).

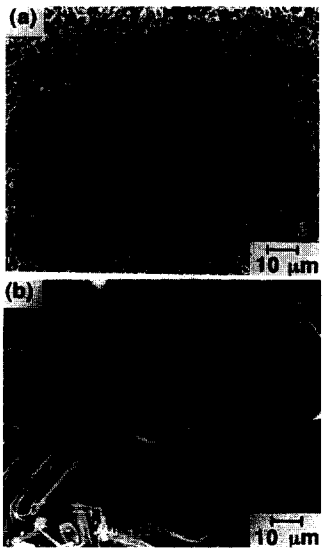

Fig. 3. SEM images of the unirradiated area (a) and the irradiated area (b) of the boride layer.

Fig. 4 shows X-ray diffraction patterns for both unirradiated area (a) and irradiated area (b). The numbers in the

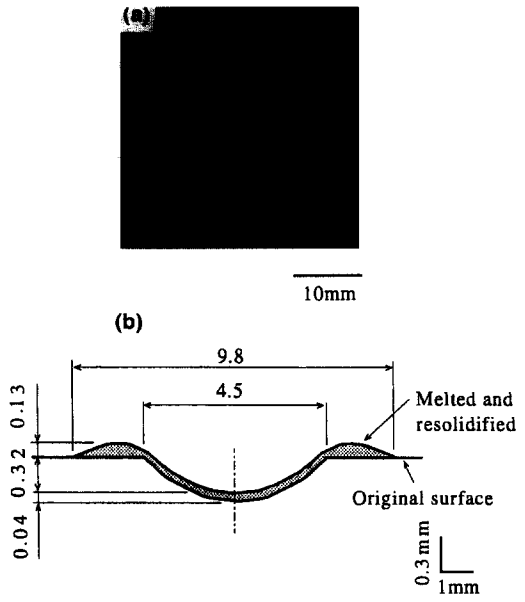

Fig. 2. Surface morphology of the irradiated boride layer (a) and the sketch of cross-sectioned surface (b).

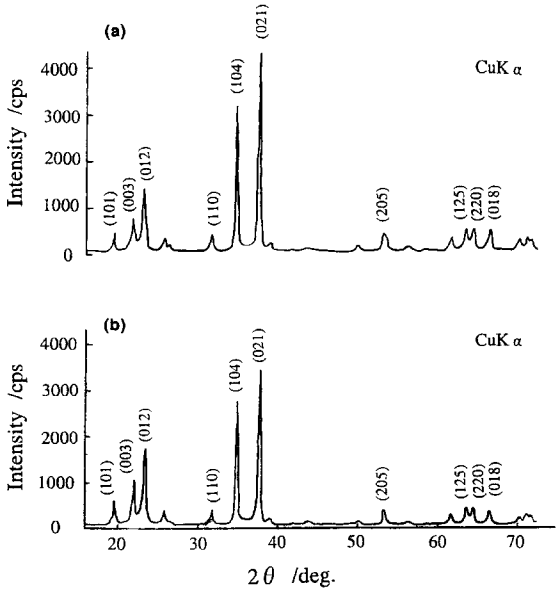

Fig. 4. X-ray diffraction pattern of the unirradiated area (a) and the irradiated area (b) of the boride layer.

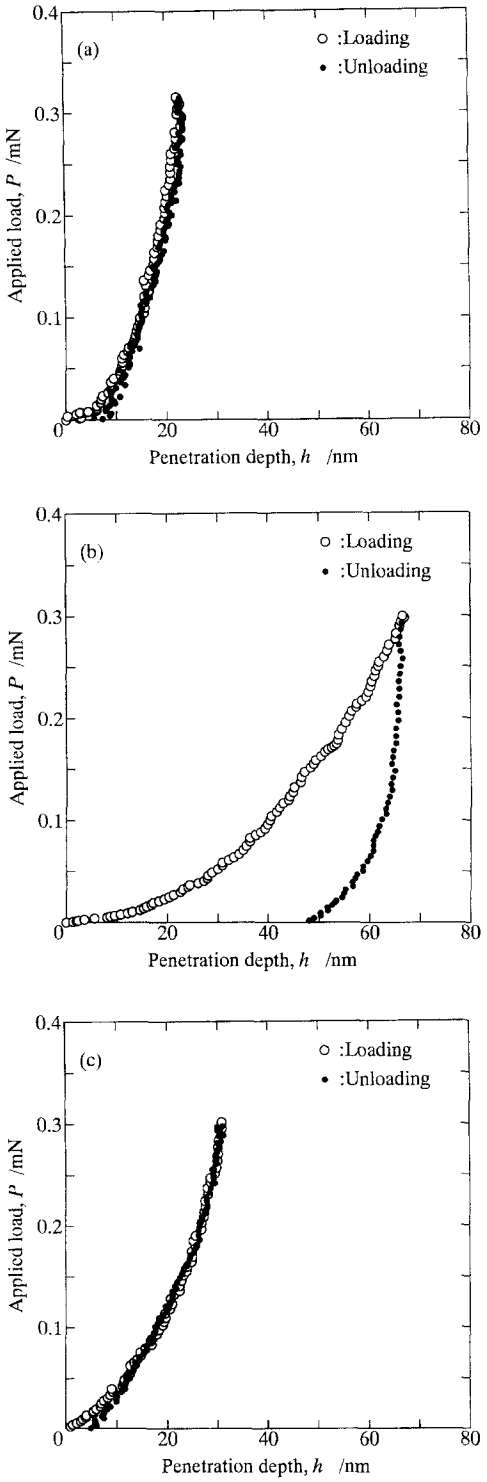

Fig. 5. Nano-indentation curves with the maximum load of 0.3 mN. (a) Standard B_4C, (b) unirradiated boride, and (c) irradiated boride on C/C.

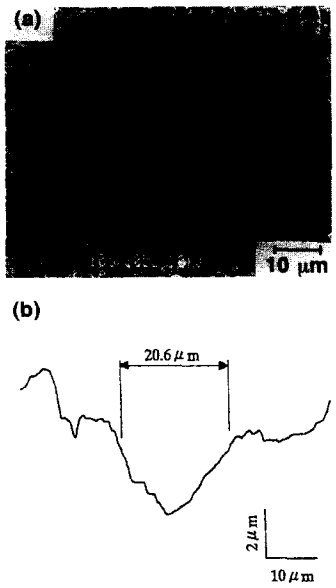

Fig. 6. Vickers hardness test in the unirradiated area at 50 gf: (a) SEM image of indentation and (b) schematic cross-sectional profile obtained from SEM observation.

figure represent Miller indices of rhombohedral structure of B_4C. The comparison between the two patterns indicates that the B_4C crystalline structure was not changed by the irradiation. Nakamura et al. [3] obtained similar results from the X-ray diffraction analysis of a low-pressure plasma-sprayed C/C composite irradiated with an electron beam under the normal heating condition. They pointed out that the boron/carbon content ratio, which was found by the electron microprobe analysis, would change at the very surface of the boride layer.

3.2. Indentation test

Fig. 5 shows typical nanoindentation curves for bulk B_4C (a), unirradiated area (b) and irradiated area (c) of the composite with a maximum applied load of 0.3 mN. The bulk and the irradiated B_4C behave elastically, while the unirradiated B_4C was elastic–plastic. The average and standard deviation for the Young's modulus and mean pressure estimated in the present study are summarized in Table 2. Here, the Young's moduli of the bulk B_4C and irradiated area of the composite are obtained by fitting the appropriate loading curves to the theoretical curve expressed by Eq. (4), and that of unirradiated area of the composite by fitting the initial unloading stiffness to the relation in Eq. (2) on the assumption that $C_A = 2/\pi^{1/2}$, $(A_a/A_r)^{1/2} = 0.63$ and $\nu_s = 0.18$ [10]. Young's modulus of the bulk B_4C obtained by the nanoindentation almost coincides with the value from the tensile test, as indicated in Table 1, whereas the mean pressure is about 20% lower

Table 2
Estimated Young's modulus and mean pressure

Material	Young's modulus E (GPa)		Mean pressure p_m (GPsa)	
	average	std. deviation	average	std. deviation
Bulk B_4C	431	125	24.2	3.24
Boride, Unirrad.	125	23.7	3.10	0.644
on C/C, Irrad.	270	99.0	19.2	4.56

than the Vickers hardness value. The slightly lower value of mean pressure is believed to be due to the fact that the estimation included the elastic deformation. Young's modulus and mean pressure of the unirradiated area are only one third and one tenth of the respective value of the bulk B_4C. These low values would originate in the porous structure of the material as is shown in Fig. 3(a), i.e., the destruction of the pores during the indentation process. Fig. 6 shows a topographic SEM image of the surface of the unirradiated area after a Vickers indentation at 50 gf (a) and its cross-sectional profile (b). The mean pressure was calculated as 1.2 GPa from the width of the indentation indicated schematically in Fig. 6. This value is 40% of that obtained from the nanoindentation test. On the surface shown in Fig. 6(a) it is seen that the porous structure of B_4C was destroyed by the indenter, which would make the mean pressure lower. The Young's modulus of the irradiated area lies in between the values for the bulk and the unirradiated area, while the mean pressure is comparable to the bulk value. This implies that the densification of the porous B_4C took place significantly but not perfectly during the melting and resolidification caused by the irradiation.

4. Conclusions

Electron irradiated boride layer overlaid on C/C composite is investigated using a nanoindentation tester with the maximum load of 0.3 mN. The X-ray diffraction analysis reveals that both the unirradiated and irradiated areas of boride are of rhombohedral B_4C structure. The values of Young's modulus and mean pressure obtained by nanoindentation for the unirradiated area are only one third and one tenth of the values for the bulk B_4C, respectively. This is believed to result from the porous structure of the material. The values for the irradiated area are comparable to or slightly lower than those for the bulk, which suggests the densification of the area caused by melting and resolidification.

References

[1] S. Tanaka, K. Yokoyama, M. Akiba, M. Araki, M. Dairaku, T. Inoue, M. Mizuno, Y. Okumura, Y. Ohara, M. Seki and K. Watanabe, Rev. Sci. Instrum. 62 (1991) 761.
[2] M. Akiba, M. Araki, M. Dairaku, K. Fukaya, T. Horie, H. Takatsu, S. Tanaka, K. Watanabe and K. Yokoyama, Proc. IEEE Symp., Fusion Eng. 13 (1990) 529.
[3] K. Nakamura, M. Akiba, S. Suzuki, K. Yokoyama, M. Dairaku, T. Ando, R. Jimbou, M. Saidoh, K. Fukaya, H. Bolt and J. Linke, J. Nucl. Mater. 196–198 (1992) 627.
[4] J.B. Pethica, R. Hutchings and W.C. Oliver, Philos. Mag. A 48 (1983) 593.
[5] J.L. Loubet, J.M. Georges, J.M. Marchesini and G. Meille, J. Tribology 106 (1984) 43.
[6] M.F. Doerner and W.D. Nix, J. Mater. Res. 1 (1986) 601.
[7] G.M. Pharr, W.C. Oliver and F.R. Brotzen, J. Mater. Res. 7 (1992) 613.
[8] I.N. Sneddon, Int. J. Eng. Sci. 3 (1965) 45.
[9] Y. Murakami, K. Tanabe, M. Itokazu and A. Shimamoto, Philos. Mag. 69 (1994) 1131.
[10] M. Kanari, K. Tanaka, S. Baba and M. Eto, Carbon, to be published.